Rotational diffusion of colloid spheres in concentrated suspensions studied by deuteron NMR

J. Kanetakis,* A. Tölle,† and H. Sillescu
Institut für Physikalische Chemie, Johannes Gutenberg-Universität Mainz, 55099 Mainz, Germany
(Received 28 May 1996)

We present a study of the application of deuteron-nuclear magnetic resonance spectroscopy (NMR) to the investigation of the rotational diffusion of spherical colloidal particles. We performed NMR pulse experiments on colloidal suspensions of polystyrene latex spheres in water-glycerol mixtures in a wide range of particle volume fractions ϕ from the dilute suspension up to $\phi=0.504$. We have analyzed the stimulated echo NMR signal in the time domain. The full shape of the orientational correlation function deviates from an exponential behavior in the whole ϕ range examined. We evaluate the rotational diffusion coefficient and calculate its ϕ dependence up to the ϕ^2 term in view of the theory proposed recently [V. Degiorgio, R. Piazza, and R. B. Jones, Phys. Rev. E **52**, 2707 (1995)], which considers the effect of two- and three-body hydrodynamic interactions upon particle reorientation. We find considerable slowing down of sphere reorientation for $\phi\geqslant 0.2$. The agreement between experimental results and theoretical considerations is satisfactory. [S1063-651X(97)02502-6]

PACS number(s): 82.70.−y

I. INTRODUCTION

Translational and rotational diffusion in colloidal dispersions has been investigated using various light scattering techniques [1–6]. In concentrated systems, the colloid particles are generally index matched with the fluid, and the light scattered from tracer particles is analyzed. The tracers become observable by different index of refraction [2], or by labeling with fluorescent [3] or photochromic dye [4] molecules attached to the colloid particles. In order to study the rotational diffusion by light scattering, the particles must be optically anisotropic. In principle this can be done with dye labeled spheres if the photobleaching reaction occurs with linearly polarized light which creates orientational order in the ensembles of unbleached and bleached dye molecules (optical Kerr effect). Since the dye molecules are rigidly bound to the colloid spheres their rotational diffusion results in depolarization of the fluorescent or scattered light in the fluorescence recovery after photobleaching (FRAP) [5], or forced Rayleigh scattering (FRS) [6] techniques, respectively. Whereas the FRAP technique has been used for studying molecular reorientation in liquids and viscous systems, we have recently applied FRS to rotational diffusion of labeled colloid spheres in a glass forming liquid [6].

The application of dynamic depolarized light scattering (DDLS) to rotational and translational diffusion of colloid spheres has become possible with fluorinated polymers where the partially crystalline internal structure gives rise to a significant depolarized component in the scattered light field [7]. Since the colloids could be index matched in aqueous urea solutions it was possible to determine the polarized and depolarized self-intermediate scattering functions in concentrated suspensions with sphere volume fractions up to $\phi=0.53$ [1].

In nontransparent dispersions the application of light scattering is reduced to backscattering techniques which have been used for studies of translational diffusion [8]. As an alternative to light scattering we have recently proposed a deuteron NMR stimulated echo technique which is common in ''ultraslow'' molecular reorientation in polymers and supercooled liquids close to the glass transition. Results on rotational diffusion of deuterated colloid spheres on a time scale of 10^{-3}–1 s have been published in a recent paper [9], where the system which was investigated was a suspension of colloid spheres in the viscous liquid phenolphthaleindimethylether (PDE). ^{13}C chemical shift anisotropy has been used as a probe of rotational Brownian motion of spherical poly(methyl methacrylate) particles suspended in water [10] at a relatively low colloid concentration of about 10 wt %. Enrichment of the particles with 20% of the isotope ^{13}C has been necessary in the two-dimensional exchange NMR experiments reported in [10].

It is the purpose of this article to give an extensive description of the possibilities and the limitations of the NMR techniques, to present results on rotational diffusion of deuterated polystyrene (PS) latex spheres suspended in water-glycerol mixtures in an extensive concentration regime (volume fractions $0.046\leqslant\phi\leqslant 0.50$), and finally to compare the rotational diffusion data with recent theoretical considerations [1].

II. NMR TECHNIQUES

Since the rotational Brownian motion of colloid spheres in a low viscosity medium occurs typically on the millisecond time scale, only the so-called ''ultraslow motion'' NMR techniques are applicable [11,12]. Here one observes the reorientation of anisotropic spin coupling tensors (e.g., the chemical shift anisotropy in ^{13}C NMR or the nuclear quadrupole coupling tensor in ^{2}H NMR) during a ''mixing time'' which separates the preparation and detection periods of particular spin states. The NMR signal detected has the form of a ''stimulated echo'' which is often analyzed as a two-

*Author to whom correspondence should be addressed.
†Current address: Institut Laue-Langevin, B. P. 156, F-38042 Grenoble Cedex, France.

dimensional (2D) NMR spectrum after time to frequency Fourier transformation. In particular, ^{13}C and ^{2}H 2D NMR have found wide application in studies of ''ultraslow'' segmental motion in solid polymers and systems close to the glass transition [12]. In principle these techniques should also be applicable to rotational diffusion of solid polymer lattices in colloid dispersions. However, the information upon the reorientation mechanism contained in the full shape of a 2D spectrum is not necessary in colloids which are known to reorient by small angular step rotational Brownian motion. (This has been confirmed for small colloid spheres with a radius of only 18 nm [9].) Therefore it is more appropriate to analyze the NMR signal in the time domain where the stimulated echo amplitude can be formulated as follows [12,13]:

$$F(\tau_1,\tau_2)=\langle\exp[-i\tau_1\omega_I(0)]\exp[i\tau_1\omega_I(\tau_2)]\rangle \times\exp(-2\tau_1/T_2)\exp(-\tau_2/T_1'), \quad (1)$$

$$\omega_I(\tau_2)=C_I\{\tfrac{1}{2}[3\cos^2\theta(\tau_2)-1]-\eta_I\sin^2\theta(\tau_2)\cos2\phi(\tau_2)\}. \quad (2)$$

Chemical shift anisotropy ($I=\frac{1}{2}$; ^{13}C, ^{19}F, ^{31}P, etc.):

$$C_{1/2}=-\omega_0\sigma_{zz}. \quad (3)$$

Nuclear quadrupole coupling ($I=1$; ^{2}H):

$$C_1=3e^2Qq/4\hbar. \quad (4)$$

The brackets $\langle\ \rangle$ denote an ensemble and orientational average. τ_1 and $\tau_2\gg\tau_1$ are, respectively, the time distances between the first and second, and between the second and third radiofrequency (rf) pulses of the Jeener stimulated echo three pulse sequence. Whereas τ_2 is the ''mixing time'' which is varied typically between 5×10^{-4} and 2 s in our experiments, the ''evolution time'' τ_1 is chosen sufficiently small in order to attain the limit (see below)

$$|\tau_1\omega_I(\tau_2)|\ll\pi/2. \quad (5)$$

In Eq. (1) T_2 is the spin-spin relaxation time ($T_2\sim300\ \mu$s for ^{2}H NMR in solids) and T_1' is the spin-lattice relaxation time where the prime indicates that $T_1'=T_{1Q}$ refers to relaxation of the quadrupolar order in the ^{2}H experiments discussed below, whereas it is the conventional spin-lattice relaxation time for nuclear spins with $I=\frac{1}{2}$. In Eq. (2), η_I is the asymmetry parameter of the anisotropic coupling tensor, i.e., $\eta_{1/2}=(\sigma_{yy}-\sigma_{xx})/\sigma_{zz}$ for chemical shift anisotropy. Whereas $\eta_{1/2}$ is finite in many organic molecules, $\eta_1\approx0$ is usually a very good approximation in the ^{2}H NMR. Thus we shall assume

$$\omega_1(\tau_2)=\omega_Q(\tau_2)=(3e^2Qq/4\hbar)P_2(\tau_2), \quad (6)$$

$$P_2(\tau_2)=\tfrac{1}{2}[3\cos^2\theta(\tau_2)-1] \quad (7)$$

in the following. $P_2(\tau_2)$ is the second Legendre polynomial and θ is the angle of the C–^{2}H bond with the external magnetic field direction. Furthermore, we chose the ''spin-alignment'' pulse sequence where a phase shift of $\pi/2$ is introduced between the first two rf pulses and Eq. (1) becomes in the limit of small τ_1 [13]

$$\begin{aligned}F_{ss}(\tau_1,\tau_2)&=\langle\sin[\tau_1\omega_Q(0)]\sin[\tau_1\omega_Q(\tau_2)]\rangle\\&\quad\times\exp(-2\tau_1/T_2)\exp(-\tau_2/T_{1Q})\\&=\langle P_2(0)P_2(\tau_2)\rangle\tau_1^2C_1^2\exp(-2\tau_1/T_2)\\&\quad\times\exp(-\tau_2/T_{1Q}).\end{aligned} \quad (8)$$

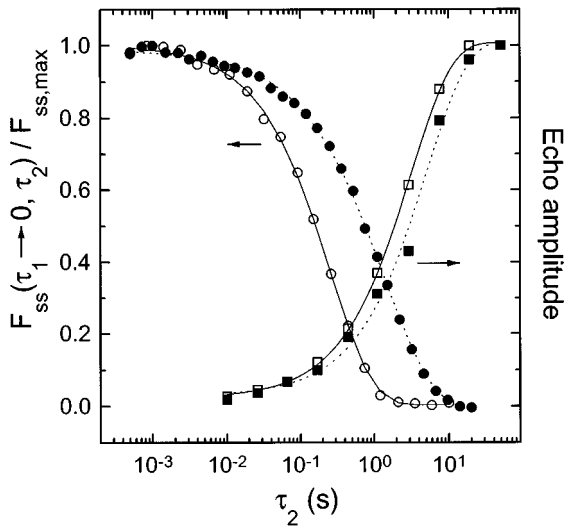

FIG. 1. Left: Normalized spin-alignment echo decay functions plotted as a function of the mixing time τ_2 between the second and third radiofrequency pulses of the stimulated echo sequence for the sample with volume fraction $\phi=0.504$ at two temperatures. ●, 233.8 K; ○, 253 K. The lines are fits to stretched exponentials $\exp[-(\tau_2/T_{1Q})^{\beta}]$ with $\beta=0.67$, 0.77 and the mean T^{1Q} values are 1.8 and 0.3 s for 233.8 and 253 K, respectively. Right: Normalized echo amplitude (magnetization) of a typical solid echo experiment plotted as a function of the buildup time of the echo. ■, 233.8 K; □, 253 K. The lines are fits to stretched exponentials with $\beta=0.79$ and the mean T_1 values are 5.8 and 3.6 s for 233.8 and 253 K, respectively.

In Fig. 1 we compare the spin-alignment echo amplitude $F_{ss}(\tau_1\rightarrow0,\ \tau_2)$ with the magnetization in a conventional ''saturation recovery'' (solid echo) experiment for determining T_1 at two low temperatures where the spin-alignment decay is dominated by the term $\exp(-\tau_2/T_{1Q})$ of Eq. (8). At 233.8 K the sphere rotation is essentially frozen; thus $T_{1Q}=1.8$ s and $T_1=5.8$ s determined from the dashed lines in Fig. 1 are identical with those in solid deuterated polystyrene (PS-d_8). It should be noted that the experimental curves were fitted with stretched exponentials, $\exp[-(t/\tau)^{\beta}]$, since spin-lattice relaxation of ^{2}H in solid glasses is nonexponential. The values of T_{1Q} and T_1 given above are averages determined as $\langle\tau\rangle=\tau\beta^{-1}\Gamma(\beta^{-1})$, where Γ denotes the gamma function and $\beta=0.67$ and 0.79 for T_{1Q} and T_1, respectively. It is well known that $T_{1Q}<T_1$ in deuterated solids, however, the ratio T_{1Q}/T_1 depends upon the nature of angular librations of the C—^{2}H bonds and is influenced by spin diffusion effects [14]. In the following we will assume that the ratio $T_{1Q}/T_1=0.3$ and $\beta=0.8$ determined at 233.8 K are approxi-

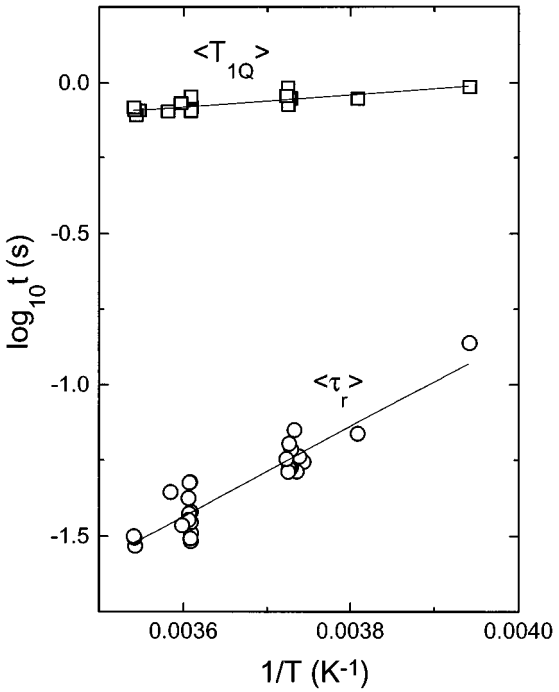

FIG. 2. Logarithm of the mean time for reorientation $\langle \tau_r \rangle$ [Eqs. (9) and (12)] and relaxation $\langle T_{1Q} \rangle$ (obtained from the ratio $T_{1Q}/T_1=0.3$ with measured T_1) plotted as a function of inverse temperature T^{-1} for the suspensions in 1:4 weight by weight glycerol-water mixtures. Repeated symbols correspond to different volume fractions at a certain temperature. The lines are Arrhenius fits with activation energies 28.5 and 4 kJ/mol for reorientation and T_{1Q} relaxation, respectively.

mately independent of temperature, and we evaluate the rotational correlation functions of sphere reorientation from Eq. (8) as

$$G_2(\tau_2)=\langle P_2(0)P_2(\tau_2)\rangle = AF_{ss}(\tau_1,\tau_2)/\exp[-(3.33\tau_2/T_1)^{0.8}], \quad (9)$$

where $\tau_1=100$ ns was chosen sufficiently small, see Eq. (5), and A was determined by extrapolation to the limit $\tau_2 \to 0$. We have measured T_1 as a function of temperature and obtained the linear fit

$$T_1=3.2 \text{ s}-0.017(T-254) \text{ s/K}, \quad (10)$$

which was used in the evaluation of $G_2(\tau_2)$ via Eq. (9). At 253 K the decay of $F_{ss}(\tau_1,\tau_2)$ is still dominated by T_{1Q} and only a rough estimate of ~ 0.3 s is obtained for the decay time of $G_2(\tau_2)$. At $T \geqslant 268$ K the sphere rotational correlation times are much shorter than T_{1Q}. The T_1 term in Eq. (9) is then only a small correction to the long-time behavior of the decay function.

In Fig. 2 we summarize the pertinent time scales for reorientation and T_{1Q} relaxation for the suspensions in glycerol-water mixtures (1:4 weight by weight ratio, see below). The temperature dependence of T_{1Q} is weaker than that of reorientation and the separation of the time scales is more than a decade at temperatures above 260 K. An Arrhenius fit to the data of Fig. 2 gives activation energies 28.5 and 4 kJ/mol for reorientation and T_{1Q} relaxation, respectively.

III. EXPERIMENTAL RESULTS

A. Sample preparation

Deuterated polystyrene (PS-d_8) latices were prepared by soap-free emulsion polymerization in water at 343 K using potassium persulfate as initiator (0.5% of diisopropenylbenzene was also added as a crosslinking agent [15]). After stabilization with the commercial nonionic surfactant Lutensol AT 25 (BASF), homogenization by ultrasound and filtration, the emulsion was concentrated by reverse osmosis. Glycerol was added in order to avoid freezing and obtain an approximate density match between the latices and the liquid, which was achieved with a 1:4 weight by weight ratio of glycerol and water. Sedimentation has not been observed; samples left for several days and measured again have shown identical correlation times and the same shape of the decay curve. The PS-d_8 emulsion with 37.2 wt % solids (gravimetric determination) was subsequently diluted by adding further amounts of glycerol-water mixture. Eight samples have been prepared with 1:4 glycerol-water mixture with weight fractions (solid basis) (in parentheses the corresponding volume fraction): 0.372 (0.356), 0.310 (0.295), 0.261 (0.248), 0.201 (0.191), 0.181 (0.171), 0.132 (0.125), 0.084 (0.079), 0.049 (0.046). In addition, two samples with 1:1.79 glycerol-water content and weight fractions (in parentheses the corresponding volume fraction) 0.512 (0.504), 0.167 (0.163) were used. The concentrated sample (0.512 weight fraction) was prepared from the remaining small amount of the 37.2 wt % stock emulsion by slow water evaporation (hence higher glycerol content) over P_2O_5 in a desiccator. A part of this concentrated sample has been diluted with 1:1.79 glycerol-water mixture to make the 0.167 weight fraction sample, which has been used as a control sample (see below). For the most concentrated sample the estimated error in weight fraction is approximately $\pm 5\%$ since only a small amount of water has evaporated. After filling in with the suspensions, the NMR sample tubes (6 mm diameter, ~ 2 cm length) were flame sealed while keeping them in liquid nitrogen to avoid evaporation.

Viscosities of the water-glycerol mixtures were obtained using a Bohlin Rheometer at shear rates 18.5–146 s^{-1}. The temperature dependence of the 1:4 glycerol-water mixture is $\ln \eta = -2.9 + \{444.46/[T(\text{K}) - 163.72]\}$ mPa s in the range from 262.6 to 313.2 K. Below 259 K the mixture seems to crystallize. The measured viscosities are in reasonable agreement with literature data [16], which, however, were taken at temperatures above 273.2 K.

B. Characterization

Particle sizes were measured with static light scattering (SLS) and dynamic light scattering (DLS). Light scattering measurements were performed at 293 K on dilute dispersions in water at a volume fraction of about 10^{-4}. Prior to measurement the samples were filtered through 1 μm Millipore filters to remove dust from the suspensions. The particles were assumed to be spherical. Particle form factors were analyzed under the Rayleigh-Gans-Debye (RGD) approximation [17] which is strictly valid for particles satisfying the RGD criterion

$$P \equiv (4\pi/\lambda)\overline{R}\Delta n \ll 1, \quad (11)$$

where Δn is the difference between the refractive index of the particles and that of the suspending liquid and R is the particle mean radius. Under these assumptions the optical particle radius R_0 was obtained from a fit of the measured scattering intensity to the RGD form factor as a function of the scattering angle ϑ ($30° \leqslant \vartheta \leqslant 120°$) at 2° intervals. The scattering intensity profile shows a shallow minimum corresponding to a polydispersity $\sigma = (\overline{R^2}/\overline{R}^2 - 1)^{1/2} \approx 0.13$ and optical radius $R_0 = 220 \pm 29$ nm. We are aware that for colloidal polystyrene in water, $\Delta n \approx 0.27$ so that $P > 1$ for the 220 nm particles and that, instead, the form factors calculated from the Mie scattering theory should be employed. However, the radius obtained from SLS is in reasonable agreement with the dynamic light scattering and the NMR results (see below).

Dynamic light scattering results were obtained using a Nd-YAG (YAG denotes yttrium aluminum garnet) laser (ADLAS, Bremen, FRG) operating at 532 nm. Autocorrelation functions were measured with an ALV 5000 correlator (ALV, Langen, FRG) at scattering angles $30° \leqslant \vartheta \leqslant 120°$. The Stokes-Einstein relation was used to determine the hydrodynamic radius R_H. Diffusion coefficients and radius polydispersity were obtained from a second-order cumulant fit. The measured reciprocal diffusion coefficients if plotted against the wave vector q show the characteristic minimum and maximum at q's close to the minimum of the scattered intensity profile [18]. An average hydrodynamic radius $R_H = 219 \pm 25$ nm is obtained, in good agreement with the SLS results. The normalized second cumulants were ≈ 0.114.

C. NMR experiments

The NMR experiments have been performed on a home-built NMR spectrometer at a frequency of 40.24 MHz. Experimental details of the NMR setup have been published previously [13]. Figure 3(a), a plot of normalized time correlation functions vs the mixing time τ_2, shows the effect of suspension concentration on the decay time. By increasing the sphere content, the correlation functions shift to longer times, demonstrating the importance of hydrodynamic interactions upon sphere reorientation. Figure 3(b) shows the effect of temperature on the correlation functions of the 37.2% mother sample. By decreasing temperature the correlation functions shift to longer times due to increasing viscosity. Before analyzing these effects in more detail, let us first discuss the analysis of the decay curves. The correlation functions of Fig. 3 have been analyzed in terms of Eq. (9) with fixed $\tau_1 = 100$ ns and fixed T_1 as measured from a solid echo experiment. $G_2(\tau_2)$ has been fitted with a stretched exponential [Kohlrausch, Williams, and Watts (KWW)] decay function $\exp[-(\tau_2/\tau)^{\beta}]$ where τ is the characteristic KWW time for reorientation. In order to fit the experimental time correlation functions $F_{ss}(\tau_2)$ four parameters have been used: the amplitude A, τ, β, and a baseline. This is the minimum number of parameters needed to fit the data. The value of the stretched exponent β lies within 0.7 and 0.86 for all samples studied. The mean rotational correlation time is defined as

$$\langle \tau_r \rangle = \frac{\tau}{\beta} \Gamma\left(\frac{1}{\beta}\right) \tag{12}$$

and the rotational diffusion coefficient is accordingly

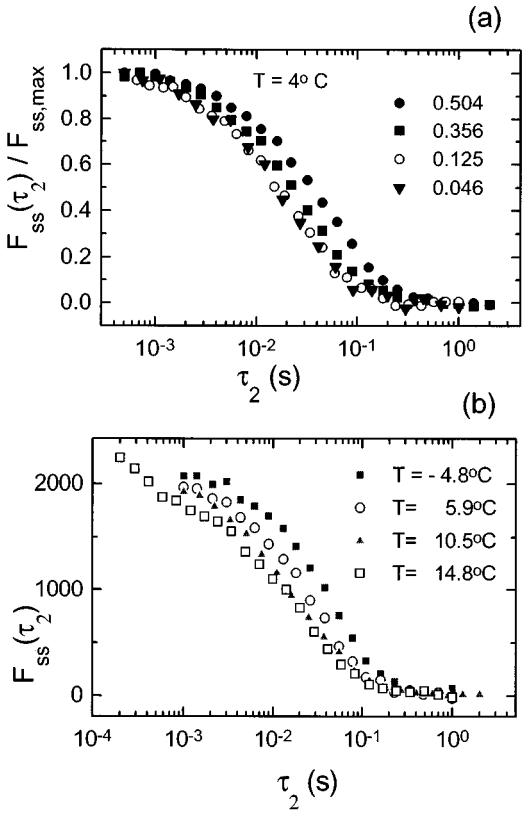

FIG. 3. (a) Normalized orientational time correlation functions [Eq. (8)] plotted as a function of the mixing time τ_2 at a temperature $T = 4$ °C for various volume fractions ϕ. (b) Orientational time correlation functions plotted as a function of the mixing time τ_2 for the sample with $\phi = 0.356$ at various temperatures. The short-time ($< 10^{-3}$ s) decay at $T = 14.8$ °C is due to spin-spin relaxation, and it can be removed by a multipulse sequence, as discussed in the text. Nevertheless the effect on the long-time orientational decay is negligible. The orientational correlation functions shown have been obtained with $\tau_1 = 100$ ns, thus fulfilling the condition $\tau_1 \rightarrow 0$.

$$D_r = (6\langle \tau_r \rangle)^{-1}. \tag{13}$$

For the most dilute sample with volume fraction $\phi = 0.046$ the analysis gives $\beta = 0.80 \pm 0.05$. This result is in contrast to the exponential decay observed in the most dilute sample ($\phi = 0.031$) of the dynamic depolarized light scattering study (Fig. 1 of [1]), where a stretched exponential fit yields $\beta = 0.97$, and the deviation from 1 is explained by the small radius polydispersity $\sigma \leqslant 0.02$. Figure 3(b) shows that at short times ($< 10^{-3}$ s) the influence of the spin-spin relaxation decay is in some cases observed. In order to exclude any T_2 effects we have applied a recently proposed multipulse sequence on the spin-alignment NMR experiment [19], thereby expanding the time window at shorter times. The results on the most dilute sample ($\phi = 0.046$) remain essentially unaltered. A second plausible explanation is the relatively high polydispersity ($\sigma \approx 0.13$) of the particles. In order to study the effect of polydispersity on the shape of the decay curves of Fig. 3, we have assumed a generalized exponential (or Schulz) particle size distribution $G(R)$ defined as [20,18]

$$G(R) = \frac{R^Z}{Z!} \left(\frac{Z+1}{\overline{R}}\right)^{Z+1} \exp\left(-\frac{R}{\overline{R}}(Z+1)\right), \tag{14}$$

where the polydispersity is related to the parameter Z by

$$\sigma^2=\frac{1}{Z+1} \tag{15}$$

and by assuming that reorientation for each particle decays exponentially with a characteristic time $\tau(R)$ depending upon size. Integrals of the form

$$S(t)=\int_{R_{\min}}^{R_{\max}} G(R)e^{-1/\tau(R)}dR \tag{16}$$

evaluated at various times t provide the decay curve $S(t)$ similar to the time correlation functions of Fig. 3. In Eq. (16), t corresponds to the mixing time τ_2 of the NMR experiment and $\tau(R)$ has been calculated from the Stokes-Einstein-Debye relation

$$\tau(R)=\frac{\eta V}{k_B T}, \tag{17}$$

where η is the shear viscosity of the suspending fluid, V is the particle volume, k_B is the Boltzmann constant, and T is temperature. Fitting of the simulated $S(t)$ curves to a stretched exponential function gives $\beta \geqslant 0.9$, for polydispersity in the range 0.14–0.2. Hence the observed β values of the experimental curves cannot be explained only on grounds of a relatively high particle polydispersity. Shape deviations (ellipticity) could have a strong influence on the rotational behavior, however, it is unlikely that the preparation followed leads to particles that deviate considerably from spherical shape. (Recent TEM micrographs of latices produced with identical polymerization techniques indicate a spherical particle shape [21].)

IV. ANALYSIS AND DISCUSSION

In a recent publication [1] the effect of hydrodynamic interactions on particle rotational diffusion has been accounted for both theoretically and experimentally using dynamic depolarized light scattering. The work reported in [1] is a considerable extension of earlier works on rotational diffusion of a tracer colloid particle in which both short- [22] and long-time orientational correlations [23] have been treated. Before analyzing our experimental findings in terms of the theory presented in [1] let us briefly summarize the main theoretical results.

The short-time rotational diffusion coefficient D_r^s of colloidal particles interacting through hard-sphere pair interactions can be written as

$$D_r^s=D_0^r H_s^r, \tag{18}$$

where D_0^r is the infinite-dilution rotational diffusion coefficient and all the direct (potential) and hydrodynamic interactions are included in the term H_s^r. Following the same practice as for the translational diffusion coefficient, H_s^r is written as a virial series in terms of volume fraction ϕ,

$$H_s^r=1+H_{s1}^r\phi+H_{s2}^r\phi^2+\cdots . \tag{19}$$

For the case of hard spheres with stick boundary conditions and with a hard-sphere pair potential, the coefficient of the linear term H_{s1}^r has been calculated from the two-body direct and hydrodynamic interactions [22] as $H_{s1}^r=-0.63$. The second-virial coefficient of H_s^r has been calculated from a combination of exact two-body contributions and three-body effects [1] as $H_{s2}^r=-0.67$ and Eq. (19) reads

$$H_s^r=1-0.630\phi-0.670\phi^2. \tag{20}$$

Combining three-body with two-body contributions (correct to the order R^{-10}) the virial expansion coefficients are [1]

$$H_s^r=1-0.500\phi-0.384\phi^2. \tag{21}$$

Although higher-order three-body interactions will slightly change the magnitude of the coefficient of ϕ^2, the second-virial coefficient of H_s^r remains negative, unlike that for translational diffusion, whose sign is changed by many-body effects [1]. Whereas for translational diffusion in concentrated suspensions the short- and long-time diffusion coefficients are effective in describing the motion of a particle within a cage of its neighbors, and the diffusion out of the cage, respectively, for rotational diffusion only the notion of the short-time rotational diffusion D_r^s is meaningful [1], since diffusion occurs on the surface of a bounded sphere.

In Fig. 4 are plotted the mean rotational correlation times calculated from Eq. (12) for the eight samples with 1:4 weight by weight ratio of glycerol and water, in the temperature range 268–288 K. The upper dashed line corresponds to the temperature dependence of η/T, where η is the zero-shear-rate viscosity of the 1:4 glycerol-water mixture, and it has been drawn to scale with the mean correlation times of the suspension $\phi=0.356$. The lower dashed line is a vertical shift of the upper one and it has been drawn to scale with the suspension $\phi=0.046$. Although the Stokes-Einstein-Debye relation, Eq. (17), is valid for dilute suspensions, Fig. 4 shows that the temperature dependence of the viscosity of the suspending medium follows the temperature dependence of the rotational correlation times even at concentrated suspensions. This result will facilitate the analysis of data taken at different temperatures and/or different water-glycerol contents. For the samples with 1:1.79 glycerol-water ratio and volume fractions 0.163 and 0.504, the reported measurements have been carried out at temperatures 18 K higher than those where the samples with 1:4 glycerol-water content have been measured, given the higher viscosity of the suspension medium. For this purpose the sample with 0.163 volume fraction (chosen as a control sample) has been measured, and its rotational correlation times have been checked against the sample with a similar solid content (0.171 volume fraction and 1:4 glycerol-water content). The agreement between the decay times measured at three different temperatures is quite good, and hence the same is expected to be true for the most concentrated sample with volume fraction 0.504.

Since the experimental curves (Fig. 3) could not be fitted by a single exponential decay, an alternative to the stretched exponential is the use of a double exponential fit. The results at a temperature $T=268.3$ K are presented in Fig. 5 (open symbols) along with the mean rotational times calculated by means of Eq. (12) (filled symbols). Applying Eq. (17) for the most dilute sample where hydrodynamic interactions are not expected to play a role would give an unreasonably low hy-

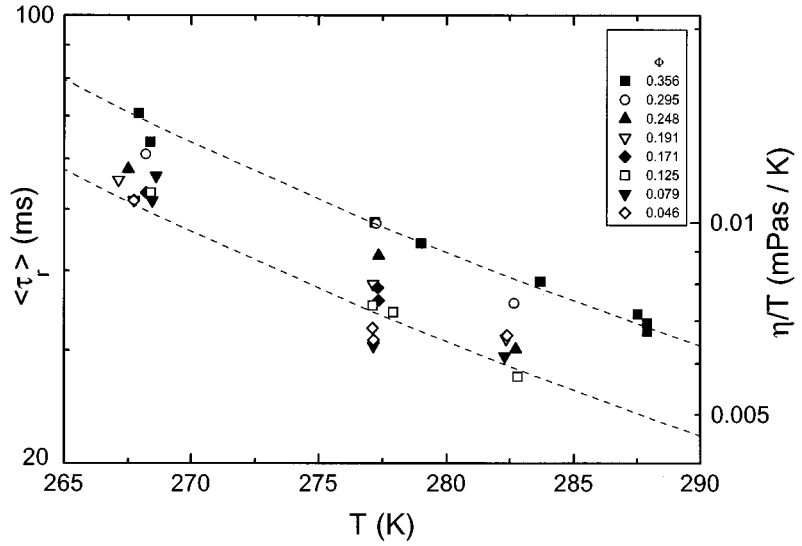

FIG. 4. Rotational correlation times $\langle\tau_r\rangle$ of the PS-d_8 spheres in 1:4 glycerol-water suspensions at various volume fractions ϕ. The $\langle\tau_r\rangle$ values have been calculated from fits to Eq. (9) of the experimental correlation functions like those depicted in Fig. 3, and represent mean values calculated according to Eq. (12). The dotted lines correspond to the measured temperature dependence of the viscosity of the 1:4 glycerol-water mixture. Upper and lower lines have been drawn to scale with the suspensions having $\phi=0.356$ and 0.046, respectively. The scale on the right refers to the upper line.

drodynamic radius if the short time is considered. The information that Fig. 5 reveals is the weak concentration dependence of the short time in comparison with the concentration dependence of the slow time, for which at the moment we can offer no explanation.

The importance of hydrodynamic interactions on the reorientation of the colloid spheres with increasing concentration can be seen in Fig. 6. The effective radius obtained from Eq. (17) using the solvent viscosity increases systematically from a volume fraction $\approx$0.2. The effective radius at low volume fractions agrees quite satisfactorily with the value of $\approx$220 nm obtained from light scattering. This further implies that the signal observed is due to reorientational motions with no influence of T_{1Q} relaxation. Parenthetically we should add that in order to get reasonable statistics, the acquisition time for the less concentrated samples has been extended over a period of days (five days are approximately needed to get one correlation function of the most dilute sample). Unlike dynamic light scattering, the correlation functions obtained are due to rotation only, since center of mass diffusion has no influence upon the NMR decay functions.

The apparent rotational diffusion coefficient D_r obtained from Eq. (13) is plotted as a function of particle volume fraction in Fig. 7. In Fig. 7(a) the values obtained at three different temperatures 267.9, 277.4, and 282.8 K are shown. The D_r data do not show a linear relation with ϕ, and the use of a second-virial coefficient in Eq. (19) is thus justified. In fact the slope of the D_r^s versus ϕ curve becomes steadily more negative with increasing particle concentration, so that the coefficient H_{s2}^r in the virial expansion must be negative. However, in the dilute regime (up to $\phi\approx$0.25) where the hydrodynamic interactions should not be very pronounced, the data can be fitted using only the first term of the virial expansion. This procedure for the data obtained at $T=267.9$ K, that show less scattering, yields $H_{s1}^r=-0.63\pm0.1$, in good agreement with the theoretical prediction [22]. This value has been fixed in the subsequent fits for the entire ϕ regime. The second-virial coefficient thus obtained amounts to $H_{s2}^r=-1.22\pm0.2$, -1.23 ± 0.1, and -1.02 ± 0.24 for 282.8, 277.4, and 267.9 K, respectively. The absolute value of the measured H_{s2}^r is higher than the theoretical value -0.67 obtained from two-body interactions, Eq. (20), and corroborates well the results of the dynamic depolarized light scattering study [1], which also found H_{s2}^r values higher than the theoretical prediction. We should bear in mind, however, that the accuracy of H_{s2}^r determined from Fig. 7(a) depends heavily on that of the sample at $\phi=0.504$ having a higher glycerol-water ratio than the other samples (see above). Nevertheless, we believe that we can exclude the value of $H_{s2}^r=-0.384$ given in Eq. (21) within the accuracy of the experimental results. From now on we will use the terms D_r and D_r^s interchangeably since we have fitted the entire correlation function to obtain D_r; however, the theoretical predictions in [1] concern rather the short-time behavior.

The D_r^s data of Fig. 7(a) measured at various tempera-

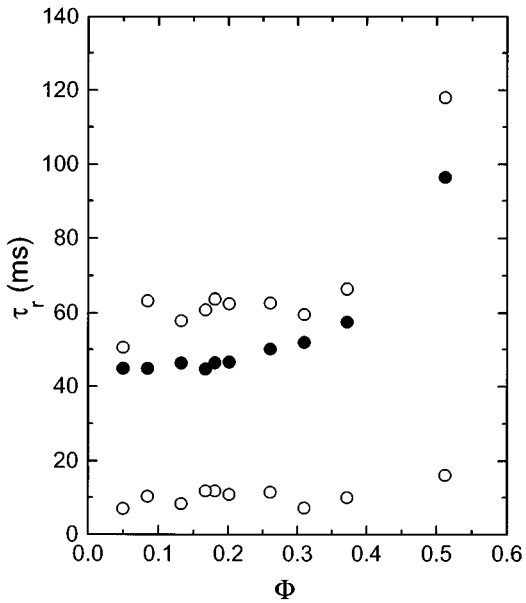

FIG. 5. Rotational correlation times τ_r plotted against volume fraction ϕ for a temperature $T=268.3$ K. Open symbols: Double exponential fit. The two open circles at a given volume fraction correspond to the two reorientational times of the double exponential fit. Filled symbol: Stretched exponential fit [$\langle\tau_r\rangle$, Eq. (17)].

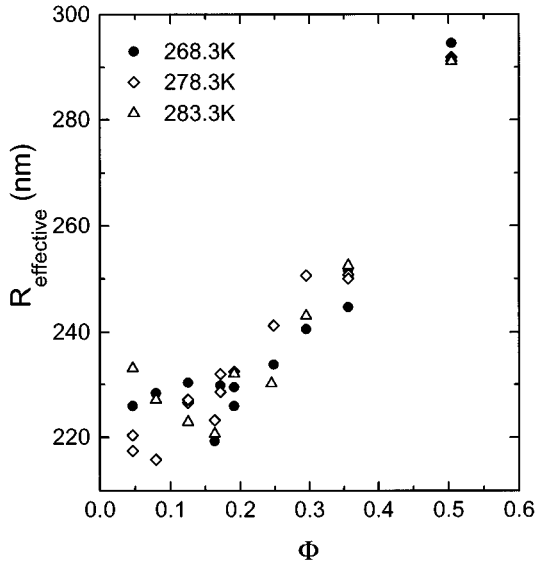

FIG. 6. Effective radius calculated by means of Eq. (17) employing the mean rotational correlation time [Eq. (12)] and the measured solvent viscosity at three different temperatures. Data at $\phi=0.163$ and 0.504 have been obtained at 18 K higher than the indicated ones due to higher glycerol-water content. For comparison, the light scattering experiments on very dilute emulsions provide a hydrodynamic radius $R_H=220$ nm.

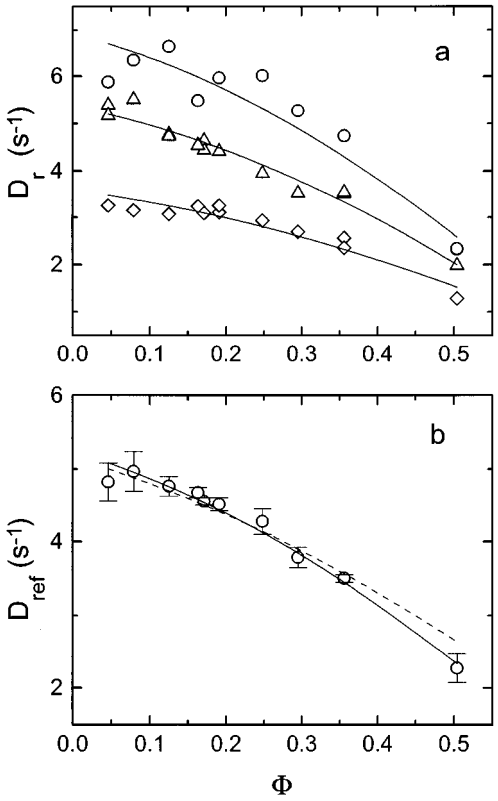

FIG. 7. (a) Rotational diffusion coefficient D_r calculated from Eq. (13) at different temperatures. ○, 282.8 K; △, 277.4 K; ◇, 267.9 K. Lines are fits to a virial expansion up to the quadratic term with $H^r_{s1}=-0.63$. (b) The data shown in (a) reduced to a temperature $T=277.4$ K. Solid line: Virial expansion with $H^r_{s1}=-0.63$ and $H^r_{s2}=-0.93$. Dashed line: Virial expansion using the theoretical prediction for hard spheres [Eq. (20)] which involves exact two-body and three-body effects. The determined second-virial coefficient $H^r_{s2}=-0.93$ is slightly higher than the theoretical prediction $H^r_{s2}=-0.67$. However, this difference is probably insignificant due to the experimental uncertainty of the D_r values. The estimated error bars in (b) are due to the statistical fluctuations in (a) but do not include the possible uncertainty due to the still unexplained nonexponentiality of the decay curves (cf. Figs. 1 and 3).

tures T can be reduced to a reference temperature T_0 by using the relation $D^s_{\rm ref}=D^s_r(\eta/T)(T_0/\eta_0)$ where the subscript 0 denotes the reference state and η is the viscosity of the suspension medium. The procedure is justified in view of the results presented in Fig. 4. We have chosen as a reference $T_0=277.4$ K, an intermediate temperature, and the result is shown in Fig. 7(b). Here the fit to the data using Eq. (19) with fixed $H^r_{s1}=-0.63$ (full line) gives

$$D^s_{\rm ref}=(5.25\pm0.05)[1-0.63\phi-(0.93\pm0.1)\phi^2]\ \ {\rm s}^{-1}. \tag{22}$$

Indeed, a free fit gives values that are hardly distinguishable from those of the constrained fit. The dashed line in Fig. 7(b) is the theoretical prediction given in Eq. (20). The agreement is rather good, especially up to $\phi\approx0.3$, although the experimental data seem to show a larger slope at higher ϕ. On the other hand, it is doubtful whether adding higher-order terms in the virial expansion would improve the agreement between theory and experiment, given the uncertainty in the parameter estimation.

The difference between the short-time rotational diffusion and the long-time behavior of the orientational correlation function has been treated in [23,1]. Here we will mention the basic features used in the analysis of our data. On theoretical grounds there exist two time scales for the orientational correlations (short [22] and long [23]). It is argued that at short times the orientational correlation function is exponential, whereas at longer times it is slowed down relative to an exponential decay due to the importance of hydrodynamic interactions [23]. A separation of these time scales from the experimental correlation functions like those depicted in Fig. 3 is not at all obvious. Hence here we have adopted as a characteristic time the mean derived from the integral of the correlation function, Eq. (12), which, according to the notation of [23], should be referred to as a long-time quantity not directly associated with the short-time rotational diffusion coefficient. The main reasoning stems from the nonexponential behavior of our experimental correlation functions, which may thus be regarded as characteristic of the long-time behavior. The long-time behavior can be expressed in terms of a virial expansion [1] as

$$\frac{G_2(\tau_2,\phi)}{G_2(\tau_2,\phi_0)}=1+(\phi-\phi_0)\gamma_2(\tau_2)+\cdots, \tag{23}$$

where $\gamma_2(\tau_2)$ measures the departure from single exponential decay, and $G_2(\tau_2,\phi_0)$ is the correlation function of the dilute (noninteracting) system. For hard spheres $\gamma_2(\tau_2)$ has been

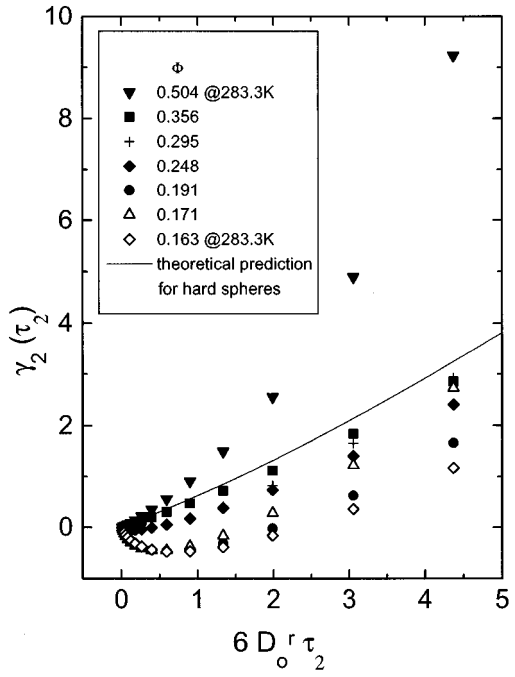

FIG. 8. Measured $\gamma_2(\tau_2)$ [Eq. (24)] plotted as a function of the dimensionless normalized time $6D_0^r\tau_2$ for various volume fractions as indicated in the inset. Measurements are reported for a temperature $T=268.3$ K, except for the volume fractions 0.504 and 0.163 which were measured at $T=283.3$ K because they have a higher glycerol content (for details see text). D_0^r is the rotational diffusion coefficient of the most dilute sample ($\phi=0.046$). The solid line represents the theoretical prediction for hard spheres at low volume fractions.

derived and computed numerically for low density suspensions in [23]. $\gamma_2(\tau_2)$ can be calculated as

$$\gamma_2(\tau_2)=\frac{G_2(\tau_2,\phi)/G_2(\tau_2,\phi_0)-1}{\phi-\phi_0}. \tag{24}$$

In Fig. 8 is shown the experimental $\gamma_2(\tau_2)$ at $T=268.3$ K for some of the measured samples relative to $\phi_0=0.046$ (our most dilute sample). The abscissa is the normalized time $6D_0^r\tau_2$ where D_0^r is the rotational diffusion coefficient of the sample with $\phi_0=0.046$. The full line represents the theoretical prediction for low ϕ [23]. If the experimental $\gamma_2(\tau_2)$ obeyed the theoretical prediction they would fall on the same curve for $\phi\leqslant 0.2$. Figure 8 shows that the experimental data underestimate the effect of hydrodynamic interactions, however, the deviation might be due to the way $\gamma_2(\tau_2)$ is calculated from the ratio of two correlation functions. Nevertheless the data show the increasing significance of hydrodynamic interactions at concentrated suspensions, especially for $\phi=0.5$.

V. CONCLUSIONS

In this work we have presented experimental results concerning rotational diffusion of polystyrene latex spheres suspended in water-glycerol mixtures. We have employed a deuteron nuclear magnetic resonance stimulated echo technique where the observable is the reorientation of the nuclear quadrupole coupling tensor. The NMR signal, in the form of a stimulated echo, has been analyzed in the time domain, and the rotational diffusion coefficient D_r has been calculated in a range of volume fractions up to $\phi=0.504$. The ϕ dependence of D_r has been compared with theoretical predictions concerning the short-time rotational diffusion, which take into account exact two-body and lowest-order three-body hydrodynamic effects [1]. We find that the predicted behavior of D_r^s is in good agreement with the experimental results. More notably, we show that the effect of hydrodynamic interactions is significant from $\phi\geqslant 0.2$. The orientational correlation functions are nonexponential in the whole ϕ range examined, an effect which cannot be fully explained by particle size polydispersity.

ACKNOWLEDGMENTS

This work has been carried out as part of the European Union Human Capital and Mobility Programme, financed by the Commission, under Contract No. ERBCHBICT930531. We thank A. Doerk for the preparation of the colloid spheres, S. Kirsch for assistance in obtaining the light scattering data, and G. Hinze for making available to us the pulse sequence for removing short-time T_2 effects.

[1] V. Degiorgio, R. Piazza, and R. B. Jones, Phys. Rev. E **52**, 2707 (1995).
[2] P. N. Pusey, in *Liquids, Freezing and Glass Transition*, edited by J. P. Hansen, D. Levesque, and J. Zinn-Justin (North-Holland, Amsterdam, 1991), pp. 763–942.
[3] A. van Blaaderen, J. Peetermans, G. Maret, and J. K. G. Dhont, J. Chem. Phys. **96**, 4591 (1992), and references therein.
[4] E. Bartsch, V. Frenz, S. Möller, and H. Sillescu, Physica A **201**, 363 (1993).
[5] M. T. Cicerone, F. R. Blackburn, and M. D. Ediger, J. Chem. Phys. **102**, 471 (1995).
[6] J. Kanetakis and H. Sillescu, Chem. Phys. Lett. **252**, 127 (1996).
[7] R. Piazza, V. Degiorgio, M. Corti, and J. Stavans, Phys. Rev. B **42**, 4885 (1992).
[8] H. Wiese and D. Horn, J. Chem. Phys. **94**, 6429 (1991).
[9] A. Tölle and H. Sillescu, Langmuir **10**, 4420 (1994).
[10] G. A. Barrall, K. Schmidt-Rohr, Y. K. Lee, K. Landfester, H. Zimmermann, G. C. Chingas, and A. Pines, J. Chem. Phys. **104**, 509 (1996).
[11] H. W. Spiess, J. Chem. Phys. **72**, 6755 (1980).
[12] K. Schmidt-Rohr and H. W. Spiess, *Multidimensional Solid-State NMR and Polymers* (Academic, London, 1994).
[13] F. Fujara, B. Geil, H. Sillescu, and G. Fleischer, Z. Phys. B **88**, 195 (1992).
[14] G. Hinze, G. Diezemann, and H. Sillescu, J. Chem. Phys. **104**, 430 (1996).
[15] M. Antonietti, R. Basten, and S. Lohmann, Macromol. Chem. Phys. **196**, 441 (1995).

[16] J. B. Segur and H. W. Oberstar, Ind. Eng. Chem. **43**, 2117 (1951).
[17] M. Kerker, *The Scattering of Light* (Academic, New York, 1969).
[18] P. N. Pusey and W. van Megen, J. Chem. Phys. **80**, 3513 (1984).
[19] G. Hinze and R. Böhmer (private communication).
[20] G. V. Schulz, Z. Phys. Chem. **43**, 25 (1935).
[21] S. Kirsch, Ph.D. thesis, University of Mainz, 1996.
[22] R. B. Jones, Physica A **150**, 339 (1988).
[23] R. B. Jones, Physica A **157**, 752 (1989).